ISSN 0016-7029, Geochemistry International, 2023, Vol. 61, No. 1, pp. 82–94. © Pleiades Publishing, Ltd., 2023.
Russian Text © The Author(s), 2023, published in Geokhimiya, 2023.

Geochemical Markers of Stagnant Zones in an Urban Heat Island

M. P. Tentyukov[a, b, *], K. A. Shukurov[c], B. D. Belan[b], D. V. Simonenkov[b], G. V. Ignatjev[d], and V. I. Mikhailov[e]

[a] *Pitirim Sorokin Syktyvkar State University, Syktyvkar, 167001 Russia*
[b] *Zuev Institute of Atmospheric Optics, Siberian Branch, Russian Academy of Sciences, Tomsk, 634055 Russia*
[c] *Obukhov Institute of Atmospheric Physics, Russian Academy of Sciences, Moscow, 119017 Russia*
[d] *Institute of Geology, Komi Science Center, Ural Branch, Russian Academy of Sciences, Syktyvkar, 167000 Russia*
[e] *Institute of Chemistry, Komi Science Center, Ural Branch, Russian Academy of Sciences, Syktyvkar, 167000 Russia*
**e-mail: tentukov@yandex.ru*

Received January 21, 2022; revised June 20, 2022; accepted June 22, 2022

Abstract—The paper presents data acquired by a comparative study of the vertical variability in the chemical composition and ratios of aerosol subdisperse fractions in snow layers chronologically correlated with the stratigraphically significant snowfall periods. These data highlight features of the concentrating of trace elements at reactive (geochemical) barriers in the snow profile. The ratio of three geochemically close groups of elements, such as siderophile, sulfophile, and lithophile elements, were found out to vary relatively little from one snow layer to another in the growing snow cover. Trajectory analysis of the transfer of air masses to which stratigraphically significant snowfalls were related to the observation site provides no evidence that the identified geochemical phenomenon can be explained by that the winter aerosol field that was formed above an urban area with different trajectories of air masses can be somehow inherited in the snow layers of the growing snow cover and thus affect the vertical distributions of trace elements. Evidence indicates that that the ratios of assemblages of trace elements in the discrete snow layers, which remain stable with the growth of the snow mass, can be employed as geochemical markers of stagnant zones in an urban heat island, and the method of geochemical sampling of a snow cover in its discrete layers at a rare network of urban meteorological observation sites is an efficient additional tool for studying microscale atmospheric processes and recovering information on characteristics of the transfer of pollutants in a spatially limited urban area.

Keywords: aerosols, dynamic light scattering, reactive barriers, urban heat island, atmospheric pollution, frost, snow cover, trace elements, long-range transport of trace elements, trajectory analysis

DOI: 10.1134/S0016702923010081

INTRODUCTION

The volume of dust–aerosol material in the troposphere nowadays continuously increases and has increased more that twofold greater over the past century (Mahowald et al., 2010). The situation is further worsened by the fact that anthropogenic activities are continuously producing new sources of aerosols that are atypical of nature. While the average fraction of anthropogenic aerosols is >10% of all aerosol particles (Ivlev, 2011), this fraction increases to 45% at industrial centers. In view of this, ecological–geochemistry assessments of urban air pollutions should take into account changes in the role of suspended particles when anthropogenic atmospheric anomalies are generated. In some situations, the composition of such anomalies is controlled by the massive fallouts of dust with relatively low concentrations of trace elements, whereas the composition of anomalies elsewhere is characterized by low dust contents and high loads of trace elements (*Environmental Geochemistry,* 1990). The territories of industrially developed population centers are contaminated unevenly, and the background of generally elevated concentrations of trace elements is complicated by clearly discernible anthropogenic anomalies that are obviously constrained to industrial facilities (*Ecological Geochemistry of Urban Landscapes,* 1995; Kasimov et al., 2016; Moskovchenko et al., 2021). The intensity of air pollution in urban areas strongly depends on the intensity of local atmospheric processes, which are triggered when an urban territory interacts with the environment. Such interactions give rise to so-called *urban heat islands*, which are discernible not only thanks to differences between the population center and adjacent "green" territories but also owing to a specific system of local circulations within the urban development areas, which control the development of processes that transfer and disperse contaminants within urban areas. It is believed that the character of the distribution of trace elements in a snow profile can sometimes be employed as markers of such processes.

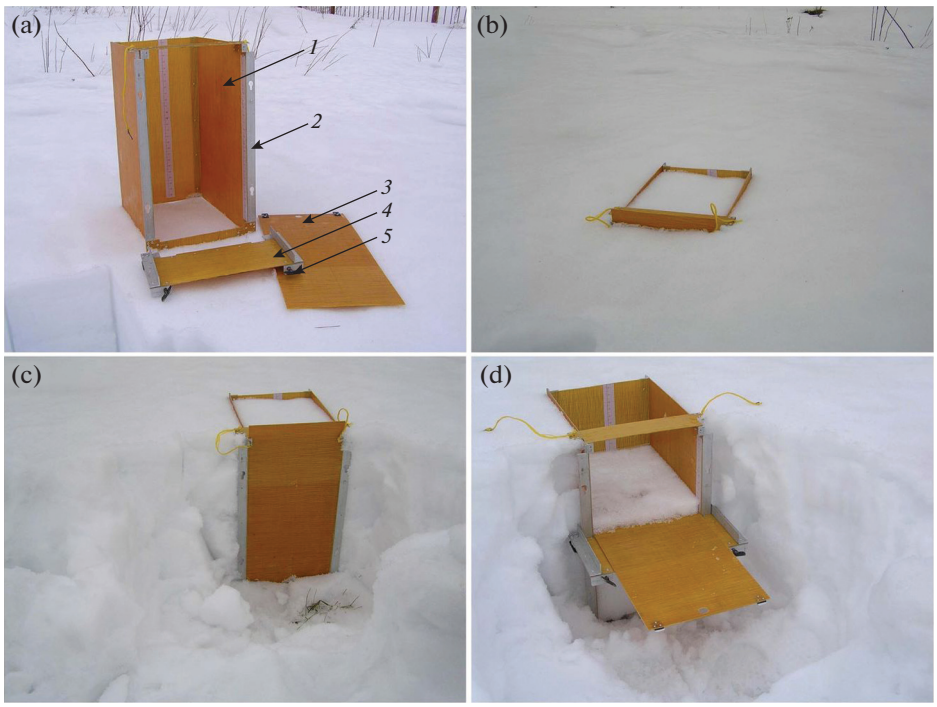

Fig. 1. Snow corer used to sample discrete snow layers and an illustration of its usage (see text for details).

Our study was focused on the effects of the origin of reactive (geochemical) barriers on the distributions of trace elements in the discrete layers of the snow cover. We also attempted to elucidate whether the distributions of the ratios of trace-element groups in discrete snow layers can be used to identify stagnant zones in an urban heat island.

METHODS

The variability in the granulometric and chemical composition of aerosol materials between discrete snow layers was studied at a snow-measuring site in the courtyard of the Institute of Geology, Komi Science Center, Ural Branch, Russian Academy of Sciences, in Syktyvkar. At this site, samples of snow from discrete snow layers were taken on February 28, 2021, with the use of a snow corer of original design (Patent 2411487..., 2011). It should also be mentioned that the snow samples were taken during an interlude between snowfalls, when the snow mass on the snow cover surface slightly increased because of frost precipitation. It was measured using a device designed for this purpose (Patent for Industrial..., 89907, 2014). The measured thickness of this newly formed loose snow layer by the time of snow sampling had been a little bit greater than 1 cm, and the total thickness of the snow cover was 71 cm.

Corer for Layer-by-Layer Snow Sampling

Figure 1a displays the device (corer) we used for sampling discrete snow layers at adjustable spacing between the sampling spots in a snow profile. The corer consists of a rectangular prism, whose walls (*1*) were manufactured of material chemically inert to atmospheric compounds deposited in the snow mass. The plates of the prism walls are fixed at reinforcement ribs (*2*), which also serve as guideways when the corer is vertically pressed into a snow cover. Snow samples were cut off with the plate knife (*3*), which was the removable front wall of the prism corer. The corer was equipped with a console platform (*4*) for adjusting the sampling spacing. The console platform was mounted onto the frontal reinforcement ribs and was equipped with fasteners (*5*) for its fixation at a desirable depth.

Sampling methods. Before snow sampling, the prism of the corer was vertically forced into the snow mass (Fig. 1b), then a pit was dug to make a free space in front of the frontal wall of the corer (*3*), and the removable console (*4*) was mounted and fixed at a desired depth of the snow bar. After this, the platform was fixed with the fasteners (5) (Fig. 1d). To take a snow sample, the frontal plate of the prism (*3*) was placed onto the console platform (*4*) and was inserted into the snow core to cut it within the prism. The snow bar thus cut off was placed, using a plastic shovel, into a polyethylene bag. On the sampling day, the samples were prepared for their analysis by weighing each sample and calculating its density (ρ, g/cm^3). The snow was then melted at room temperature, and the snowmelt water was potentiometrically analyzed for pH and conductometrically for electric conductivity (ηS, μS/cm).

The layer-by-layer variations in granulometric composition of the aerosol material accumulated in the snow mass was analyzed by dynamic light scattering (DLS) by an ZetaSizer Nano ZS (Malvern Panalytical, Great Britain) laser analyzer. This method does not require any preparatory calibration of the equipment and is equally efficient at low concentrations of particles and in the presence of their aggregates. The measurable size of the particles lies within the range of 1 to 10 000 nm. Note that this range also encompasses the whole three-level gradation of aerosols (Ivlev and Dovgalyuk, 1999): finely dispersed ($D \leq 0.1$ μm or 100 nm), intermediately dispersed ($0.1 < D < 1$ μm or $100 < D < 1000$ nm), and coarsely dispersed ($r \geq 1$ μm, i.e., ≥1000 nm). The method is relatively cheap and enables the researcher to rapidly acquire reasonably accurate analyses.

In analyzing the granulometric composition of the material, the optimal accumulation time of the correlation function for each measurement of the volumetric size distribution of the particles was automatically measured using the proprietary software of the tool. The volumetric content of nanoparticles in samples was calculated integrally from the ratio (in %) of the areas under the curves describing the size distribution of the particles in linear coordinates.

The quantitative chemical composition of the snowmelt water was analyzed in samples that had been preparatorily centrifugated to get rid of suspension particles. The samples were analyzed by ICP-MS on a Agilent 7700x (Agilent Technologies, United States).

The trajectory analysis of the transfer of air masses to Syktyvkar, a process that forms the wintertime aerosol field, was carried out by the concentration weighted trajectories technique (CWT; Hsu et al., 2003), using seven-day backward trajectories, which were calculated by the method (Shukurov et al., 2018), the NOAA HYSPLIT_4 trajectory model (Draxler and Hess, 1998), and the NCEP/NCAR Reanalysis meteofields (Kistler et al., 2001). The probability field of air transport toward the city was calculated by the method (Shukurov and Chkhetiani, 2017).

RESULTS AND DISCUSSION

Formation Characteristics of the Snow Cover in Winter 2020–2021

The first snow fell in the area on October 10, and the snow depth was 4 cm. On March, 11, relatively warm weather came, with a daily mean temperature of +3°C and with alternating raining and sleeting, which had increased the snow height to 6 cm by December, 11 (Fig. 2a).

In spite of snowfalls during the following days, the snow cover grew slowly because of the positive temperature at daytime, with the snow that fell at nighttime melting and settling during daytime. A sustainable growth of the snow cover recurred on November, 21, and the snow depth had reached 11 cm by November, 27. After that, the snowfalls were infrequent and not heavy (Fig. 2b), and the depth of the snow cover grew slowly. By the time of the first warming on December 21 through 23, the height of the snow cover had been 29 cm. At that time, a relatively warm weather came (the mean daily temperature was close to 0°C), with precipitation in the form of sleet and rain. Because of this and despite the heavy snowing (Fig. 2b), the snow cover depth decreased to 28 cm. The temperature decreased after December, 23 (from 0 to −13°C). The winter freezing weather that came afterward and the frequent snowfalls resulted in the rapid growth of the snow cover, whose depth had reached 54 cm by the onset of the second warming on January 25 through 28. Note that the maximum air temperature during the second warming varied from +1.3 to −1.3°C, and the precipitation fell in the form of sleet with drizzle. The snow cover depth during this warming period decreased from 54 to 49 cm. After this, the trend of snow accumulation became as is typical of wintertime, and the growth of the snow cover had not been discontinued.

Textural–Structural Feature of the Snow Cover

These features are evident from Profile 27, which was studied and sampled on February 26, 2021, at the snow-measuring site in the inner courtyard of the Institute of Geology, Komi Science Center, Ural Branch, Russian Academy of Sciences, in Syktyvkar. The vertical section of the snow cover was made up of five discernible stratigraphic layers of various thickness (Fig. 3). The *first layer* was a little bit thicker than 1 cm and consisted of fresh surface frost. This layer rested on the loose *second layer* 8 cm thick. The structure of the second layer showed evidence of postsedimentation transformations of the older solid precipitation: along with fresh snow fragments, this layer contained small (<0.5 mm) roundish grains. The *third layer* was 6 cm thick and consisted of fine-grained compacted snow. The snow was compacted under the effect of a strong wind and temperature decrease. The *fourth layer* is 13 cm in thickness. It was made up of opaque aggregates of small (0.5–1.0 mm) roundish and subhedral snow grains. These crystals with edges were readily discernible in the contact zone with the *fifth layer*, which consisted of glaciated snow grains that had been formed during the January warming. Because of the optical anisotropy of the snow layers, the upper and lower contact zones were discernible quite clearly. It is thought that the mechanism that formed the horizontal layering of glaciated aggregates is related to the migration of capillary moisture. It is also believed that capillary moisture migrates from the surface of the snow grains toward lower and colder snow layers at warming to form there subhorizontal glaciated beds, whose thicknesses sometimes vary laterally. These glaciated beds are more or less permeable (Firts et al., 2012), and this feature allows them to

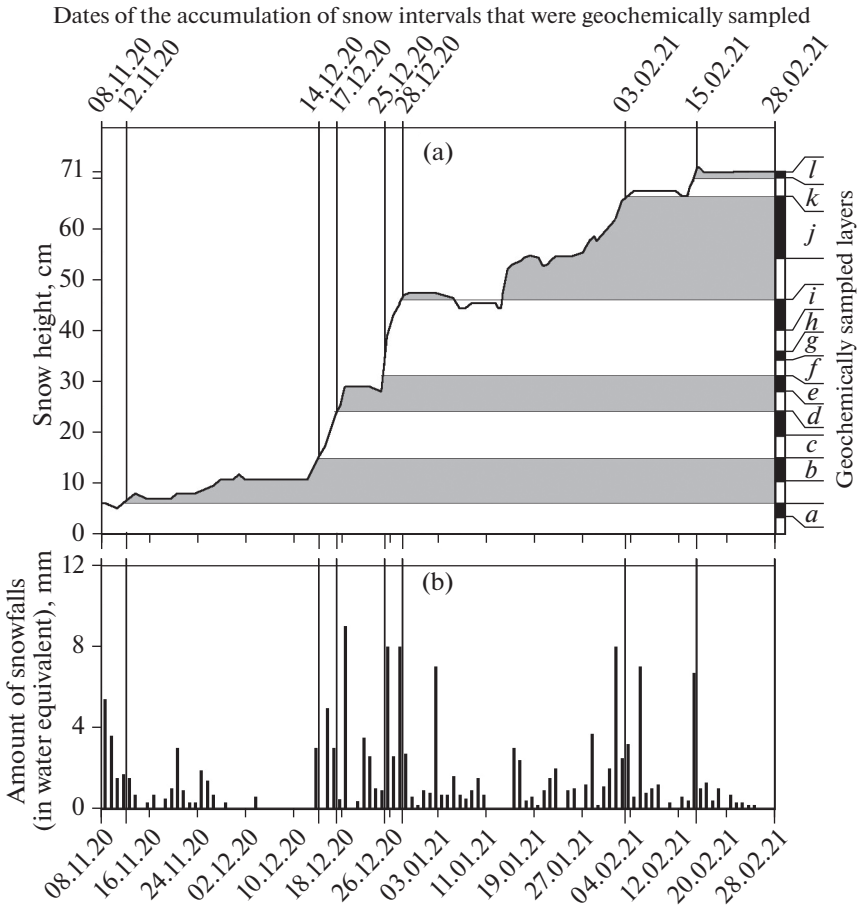

Fig. 2. Time series of the intensity of snow cover growth with (a) the layers of geochemical sampling in the snow cover, which are (b) correlated with the dates of the stratigraphically significant snowfalls (data: Syktyvkar weather station). Letter labels of the fall dates of geochemically sampled snow layers: (a) 08–12.11.20; (b) 12.11–14.12.20; (c) 14–17.12.20; (d, e) 17–25.12.20; (f, g, h, i) 25–28.12.20; (j) 28.12.20–03.02.21; (k) 03–15.02.21; (l) 15–28.02.21.

thicken within the snow cover because capillary moisture freezes over them. Such horizontal glaciated beds are thought to hamper the vertical migration of capillary moisture and are able to operate as a sort of a reactive barrier. The *sixth layer* up to 20 cm thick was composed of larger subhedral roundish grains. The coarsening of the grains was obvious near the contact with the *seventh layer*, which consisted of glaciated aggregates of snow grains. This layer was 2 cm thick and had been formed, similar to the overlying layer, during the brief warming in December. The *eighth layer* (up to 13 cm) consists of roundish subhedral grains. The *ninth layer* was a glaciated bed that had been produced during the November warming. This layer overlied the lowermost *tenth layer*, which was made up of equant crystals of deep frost (up to 3 mm). The thicknesses of the two lowermost layers were 3 and 4 cm, respectively.

Variations in Geochemical Parameters between Layers of the Snow Cover

The **hydrogen index** (pH) is an integral geochemical parameter. The pH of the snowmelt water varies from 6.2 to 7.3 (Fig. 2). Note the variability of individual pH values in the middle part of the snow cover. The difference between pH values in layers f and g is one pH unit. The differences between pH values in layers below and above this zone vary within a few tenths of a unit and tend to shift from weakly acidic to near-neutral. It should be mentioned that the maximum pH values are constrained, in addition to layers g and i, also to the upper capillary barrier, whereas the middle and lower capillary barriers in the snow profile are discernible less clearly. Note that the dynamics of the pH variations provides little information on the geochemical conditions developing in the snow profile, because pH decreases the integral characteristic of all base–acid interactions in the snow cover. Analysis of the electrical conductivity of the snowmelt water may hopefully be more informative when the snow masses are alkalinized with the precipitating aerosol material.

The **electrical conductivity of the snowmelt water** was measured conductometrically. Analysis of the vertical distribution of the snow conductivity values reveals two peaks (Fig. 3), both of which occur in snow layers in the middle part of the snow cover and are

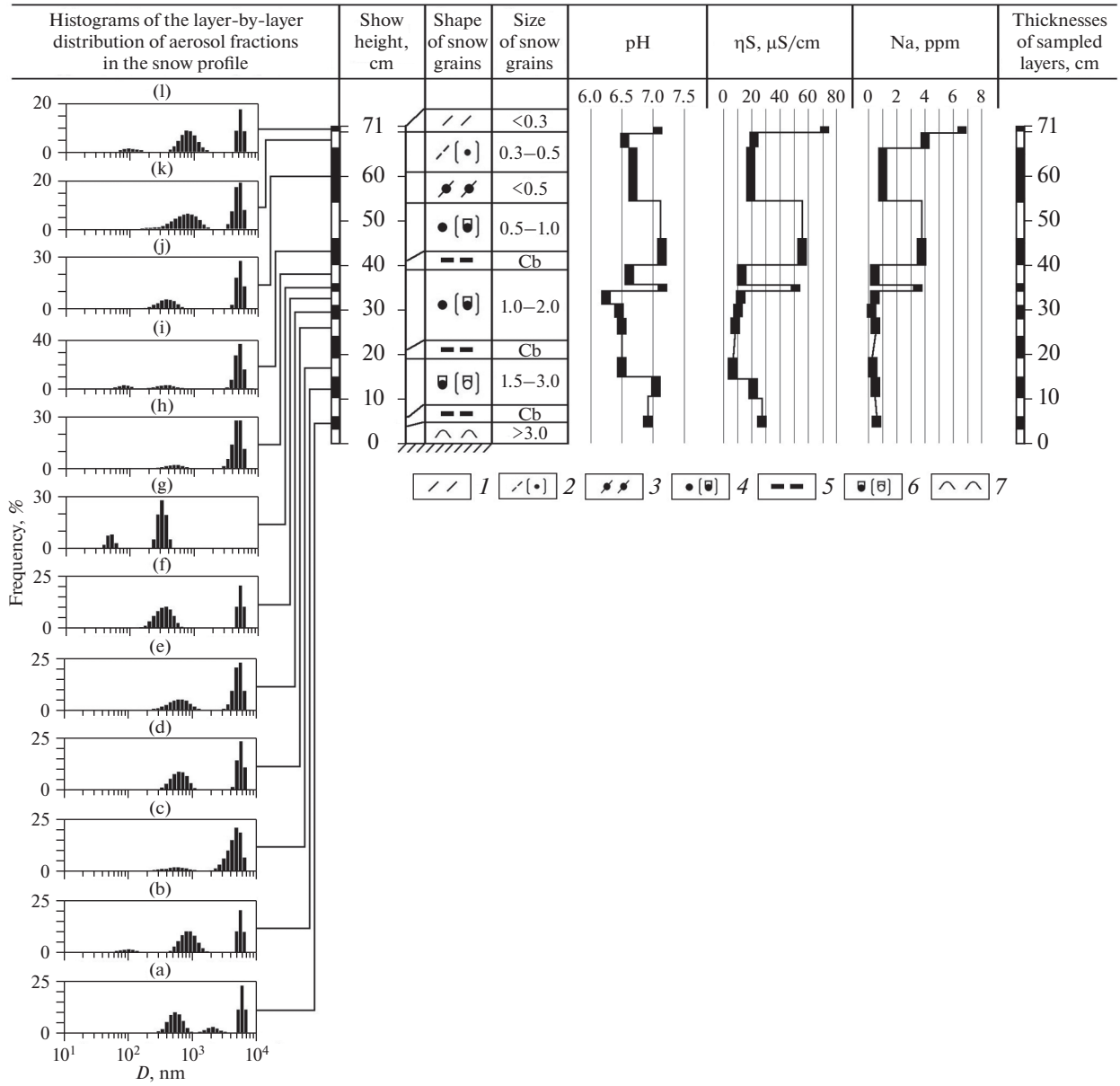

Fig. 3. Layer-by-layer Size distribution of aerosol particles in the discrete layers of the snowpack with integral indicators of the geochemical activity of the snow cover: hydrogen index (pH), electrical conductivity (ηS, μS/cm). Legend: (1) newly fallen snow (hoarfrost) (PP), (2) recently deposited snow (DFbk) with rounded grains (RGsr), (3) wind packing of fine-grained snow particles (RGwp), (4) rounded snow grains and rounded particles with edges (RGlr/RGxf), (5) horizontal glaciated layer of large snow aggregate grains (IFil), acting as a capillary geochemical barrier (Cb); (6) rounded particles with edges and rounded snow grains with edges (RGxf/FCxr) operating as a capillary reactive barrier (Cb); (7) deep frost (DHxr) (classification of grain shapes (F) is according to Firts et al., 2012).

adjacent to the capillary barrier. Simultaneous variations seen in the plots of the Na concentration and conductivity in this zone indicate that the variations in the conductivity are controlled, first of all, by changes in the Na concentrations at the reactive barriers.

We also cannot rule out that Na may be supplied by the wind transfer of ice-melting chemicals. Their fallouts onto the snow surface, together with aerosols, may increase the concentrations of easily hydrolyzed compounds. The involvement of these compounds in the reactions of low-temperature (cryogenic) complexation induces an increase in the concentration of free ions, and thus also the conductivity, in the reactive barrier zones. However, measurements of conductivity in the middle portion of the snow cover led to the discovery of a fact that is still hard to explain: a layer of low conductivity was identified between layers with high values of this parameter. This contrasting decrease in the conductivity in the capillary barrier

zone is possible if aerosol material migrates with the capillary moisture in different directions. This hypothesis requires further studies to be validated.

Frequency Distribution of Aerosol Particles in Snow Layers Chronologically Correlated with Stratigraphically Significant Snowfalls

Figure 3 shows the size distribution of sumbicrometer-sized fractions of aerosol material in the snow layers. The layers were chronologically correlated by the fall time of stratigraphically significant snowfalls (Fig. 2a). Analysis of the frequency of the size distribution of the sumbicrometer-sized particles reveals a trimodal distribution in the surface frost (layer l) and deep frost (layers a and b) and a bimodal distribution for the rest of the snow profile (layers k, j, g, h, f, e, d, and c but not layer i).

The layers with a bimodal distribution type of particles produced during snowfalls show a stable correlation of the sets with certain size ranges. For example, one was identified with gentle- and acute-top peaks with maxima within the ranges of 345–898 and 4540–5586 nm. These layers are persistently dominated by large particles: 8–48% against 42–92%. The only exception is layer g. This layer is principally different from the others in that, at its bimodal distribution, it contains much more finely dispersed fraction, which shows peaks at 55 and 345 nm. In all other layers, the content of this fraction is one order of magnitude lower. These proportions of the fractions of aerosol material in layer g reflect the postsedimentation redistribution of aerosols in snow layers adjacent to the capillary barrier as a result of the descending migration of capillary moisture. Consequently, underlying layer f is significantly enriched in the medium dispersed fraction. While the coarsely dispersed fraction dominated over the medium dispersed one in all instances discussed above, the content of medium dispersed fraction in layer f was 58%, at 42% of the coarsely dispersed fraction (at the size of the medium and coarsely dispersed fractions with clearly discernible peaks at 379 and 5590 nm, respectively).

The effect of the capillary mechanical barrier may also explain the occurrence of the finely dispersed fraction in layer i. As follows from Fig. 3, the four underlying layers (layers i, h, g, and f) are constrained to the snow horizon whose snow was accumulated very rapidly and which hosts the first capillary barrier (Fig. 2a). Thereby layer i contains all of the three size fractions of particles, whose peaks lie at 116, 394, and 5332 nm. No evidence indicates that this resulted from the precipitation of dry aerosols, because the time and character of the fallouts of the solid particles shows (Fig. 2b) that the snow cover grew at that time only because of snowfalls. It is thus reasonable to think that layer i, which was produced after the snowfalls, contained two fractions (medium and coarsely dispersed), whereas the finely dispersed one was brought by the redistribution of particles between the layers due to thermodiffusiophoresis, and the particles may have been brought from layer h. This layer is characterized by a bimodal distribution of the medium and coarsely dispersed fractions with peaks at 519 and 5045 nm, with the coarse fraction significantly dominating over the medium one: 92 and 8%, respectively. Note that the proportion of these fractions in layer j (which overlies layer i) is close to 1 : 3.

In layers with a trimodal distribution of the particles, analysis of the proportions of the dispersed fractions shows that the first fraction falls within the range of 60 to 180 nm with a gentle peak at 98 nm in the surface frost (layer l). The other two fractions correspond to broad ranges of 400–1900 to 4500–7000 nm, with clearly seen peaks at 554 and 5560 nm, respectively. Whereas the content of the finely dispersed fraction was 3%, those of the medium and coarsely dispersed ones were 46 and 51%, respectively. Layer l was formed between two snowfalls, and hence, its granulometric composition reflects features of the dry precipitation of aerosols and is related to the formation of the surface frost.

At the same time, the deep frost (layers a and b) is characterized by a trimodal distribution of the fractions. The distribution of dispersed fractions of the aerosol material in layer a is characterized by that the size range is strongly shifted rightward. Thereby one of the sets characterizes the medium dispersed fraction with a clearly pronounced peak with a maximum at 549 nm, and the other two correspond to gentle-top and acute-top peaks at 2018 and 6086 nm and pertain to the coarsely dispersed fraction. The percentages of the fractions (45, 8, and 47%, respectively) indicate that the second coarsely dispersed fraction was formed in relation to the increase in the concentration of particles in the capillary liquid because of the vertical migration of soluble compounds in the soil moisture. This hypothesis is based on that the conductivity increases in this part of the snow profile (Fig. 3). Conceivably, thermodiffusionphoresis of soil moisture vapors is sufficiently intense, because layer b, which is adjacent to layer a, contains a finely dispersed fraction with a peak at 112 nm in the range of 65–150 nm. Therewith the medium dispersed fraction lies within the range of 450–2000 nm, with an acute-top peak at 898 nm, and the coarse disperse fraction occurs within the range of 4600–7000 nm, with a clear peak at 5586 nm. The aforementioned changes in the granulometric composition of layers a and b may, perhaps, be explained by postsedimentation transformations of the aerosol material in the near-soil snow layer, in which a frost-generated (cryogenic) thermodiffusion reactive barrier is formed. It is pertinent to mention that factors favorable for the origin of reactive barriers in a snow cover are natural processes and phenomena (thermophoresis, diffusiophoresis, capillary forces, and adhesion/wettability) that are predetermined by properties of the snow profile itself.

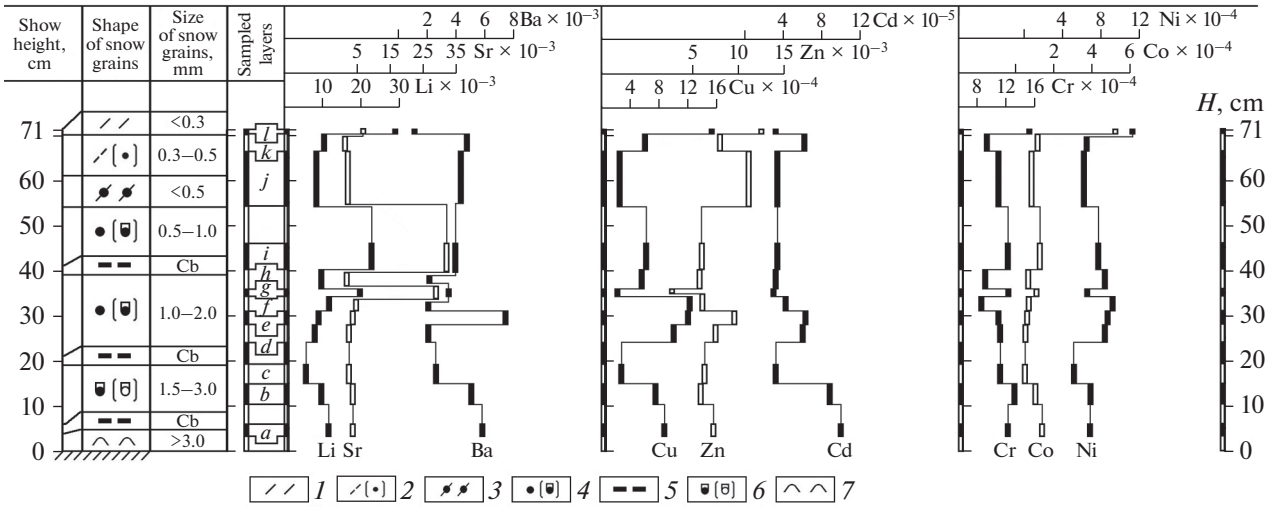

Fig. 4. Accumulation of trace elements at reactive barriers in the seasonal snow cover (the snow measuring site was located in the inner court of the Institute of Geology, Komi Science Center, Ural Branch, Russian Academy of Sciences, section 27). Legend: (1) newly fallen snow (hoarfrost) (PP), (2) recently deposited snow (DFbk) with rounded grains (RGsr), (3) wind packing of fine-grained snow particles (RGwp), (4) rounded snow grains and rounded particles with edges (RGlr/RGxf), (5) horizontal glaciated layer of large snow grain aggregates (IFil); (6) rounded particles with faces and rounded snow grains with edges (RGxf/FCxr); (7) deep frost (DHxr) [classification of grain shapes (F) is given according to Firts et al., 2012].

Specifics of the Origin of Reactive Barriers on the Snow Surface and within the Snow Cover

Data of quantitative mass-spectrometric analysis were used to plot the distribution of the concentrations of chemical elements in discrete layers of the snow profile (Fig. 4). As follows from this plot, the snow profile comprises the following three zones in which trace elements are accumulated.

The **first zone** is constrained to layer l and is characterized by enrichment in a broad spectrum of trace elements, which are accumulated at the surface thermodiffusion reactive barrier (Fig. 4), which is formed at the snow–atmosphere interface due to features typical of the accumulation of dry aerosols in wintertime. It is known that snow cover always (even at the lowest temperature) emits long-wave radiation (its own heat) and is also able to reflect much solar radiation, which facilitates the strong cooling of the snow cover and results in a temperature inversion (so-called *snow inversion*, according to Rikhter, 1948). Moreover, the surface of a snow cover is characterized not only by a high reflectivity and emissivity (Kuz'min, 1957) but also by the ability of drying the surface air (Rikhter, 1948). In the presence of temperature and moisture gradients, a snow cover receives excess moisture from the surface air and thus induces descending air migration. This results in the stable transport of water vapor toward the snow cover. This process stimulates the runoff of aerosol material from the near-surface atmosphere. The process is associated with an increase in concentrations of trace elements on the snow cover surface (Fig. 4).

The **second zone** of the accumulation of trace elements is constrained to the middle part of the snow profile, to the capillary barrier, which is, in turn, formed in the glaciated snow layer that had been produced during warmings. Note that the accuracy of the location of the mechanical capillary barrier was controlled by correlating peaks of trace elements that formed a paragenetic geochemical association, which reflects natural snow-geochemical processes that maintain the accumulation of trace elements at the mechanical capillary reactive barrier. The mechanism responsible for the accumulation of trace elements is currently thought to be regaled to the generation of clathrates.

It is known that water transition from the liquid to crystalline state takes place at exactly 0°C, but the freezing point is shifted to a lower temperature if the water contains dissolved compounds. According to the Raoult law, a decrease in the freezing point is proportional to the concentration of the dissolved compound. The cooling of a diluted solution to a temperature below 0°C should lead to ice crystallization and phase separation. A further temperature decrease should lead to an increase in the ice volume and in that the residual solution becomes progressively more concentrated, unit the eutectic concentration and temperature are reached. At this point, the dissolved compound and the rest of the solvent crystallize, and precipitate settles that consists of interlaced domains of the dissolved compound and ice, i.e., a clathrate is formed (Glinka, 1987). It is known that a determining role in its formation is played not by the reaction ability of the components but the spatial correspondence (complementarity) of the crystalline dissolved compound and pure volumetric ice.

Note that the second peak in the concentration of trace elements, which was formed below the capillary reactive barrier, is constrained to the transition layer of

the snow grains from fine- to medium-grained ones. The origin of this layer in the middle part of the snow profile is explained as follows. It is known that the temperature of a snow cover is usually lower than the temperature of the adjacent air layer because of the high albedo. This decreases the relative moisture content in the air layer and results in a deficiency of water vapor concentration in air above the snow surface. However, vapor deficit in the near-snow air layer can be counterbalanced by the ablimation of ice crystals. Because an ablimation transition from a crystalline phase into vapor is associated with heat consumption, the temperature of the uppermost snow layer decreases even further. This results in a temperature gradient in the middle part of the snow profile and in the related movement of water vapor from the lower, relatively warm, snow layers into upper colder ones.

This results in a gradient in the water vapor pressure in the upper part of the snow profile induced by the temperature gradient. Because of this, water vapor comes to the snow surface from both deeper layers and middle ones in the snow profile. However, this process in the middle part of the snow profile can be disturbed. It is known that daily variations in air temperature in dry snow with an average density of 0.28 g/cm^3 occur at a depth no greater than 50 cm and are absent below (Kuz'min, 1957). At the same time, data (Tentyukov, 2021) on the dynamics of structural–textural transformations in a freshly fallen snow layer at its transformation into a stratigraphically significant snow layer provide grounds to suggest that daily temperature variations and related possedimentation transformations of the solid precipitation should be constrained (at all other things equal) by the diffusion-controlled transfer of soil moisture in the opposite direction. This process begins in the lower part of a snow profile as a consequence of the in-snow temperature inversion (the temperature in the bottom part of a snow profile is always higher than in its middle portion). The possibility of such processes in snow profiles has been demonstrated in (Gurtovaya, 1961; Sokratov and Maeno, 2000; Sokratov, 2001; Pinzer et al., 2012). Hence, the second concentration peak of trace elements in the middle part of the snow profile is formed by the redistribution of aerosol material between the layers, which is induced by the migration of capillary moisture in the contact zone of the descending front of daily temperature variations and the ascending diffusion-controlled transport of soil moisture.

The **third zone** of accumulation of trace elements is found in the bottom part of the snow profile and, similar to what occurs in the second zone, trace elements are concentrated at the capillary reactive barrier. However, the mechanism producing it is different. It is known that soil density and, hence, its volumetric heat capacity are several times higher than those of snow (Gurtovaya, 1961). This results in a temperature gradient at the snow–soil interface, and this gradient induces an influx of subcooled pore soil solutions. This influx causes the recrystallization of the earlier snow grains and the origin of deep frost crystals. They grow further by means of repeating recrystallization, which is maintained by the continuous diffusion-controlled inflow of soil moisture. This led to the conclusion that a specific crystal-forming environment is produced in the lower part of a seasonal snow profile. This environment is characterized by certain conditions favorable for the nucleation and growth of the crystals of deep frost. These conditions include changes in the thermodynamic and physicochemical parameters. The most informative of them is pH, electrical conductivity, and density of the snow layer in the contact zone (Fig. 4). Inasmuch as the most intense vapor diffusion and the highest temperatures are usually found in the bottom part of a snow profile (Kolomyts, 2013), the ice crystals of deep frost most rapidly grow and recrystallize with the origin of clathrates exactly in the contact snow layer, whose density is relatively low, and this leads to the accumulation of trace elements in the deep frost crystals (Fig. 4). Hence, the barriers are formed and trace elements are accumulated at the thermodiffusion barrier in the lower part of a seasonal snow profile because an specific crystal-forming environment occurs in this transitional zone. Trace elements are brought into this zone by thrmodiffusiophoresis of soil moisture and dissolved soil material.

Development Features of the Winter Aerosol Field above an Urban Area and Differences in the Distributions of Trace Elements between Snow Layers

Comparison of the layer-by-layer accumulation of trace elements and the configuration of the distribution curves of these elements in the snow profile (Fig. 4) indicates that the uppermost layer l is noted for that it contains a broad spectrum of accumulated elements. However, analysis of the vertical distribution of trace elements reveals that three elements, Co–Cr–Ni, differ from the others (Li–Sr–Ba and Cu–Zn–Cd) in a more monotonous configuration of the distribution plots. It is not fully warranted to explain this fact solely by features of the postsedimentation redistribution of the aerosol material when reactive barriers are formed. It was hypothesized that, when a winter aerosol field is formed above an urban area, the trajectories of air masses to which stratigraphically significant snowfalls are related can be somehow inherited in the snow layers when the snow cover grows and can thus affect the vertical distribution of trace elements. To test this hypothesis, we conducted trajectory analysis of the atmospheric transfer of trace elements.

Analysis of the atmospheric transfer of trace elements to which the origin of the winter aerosol field above an urban area is related on snowfall days. This was done using ten-day backward trajectories of air particles which arrived hourly, starting on November 8, 2020, through March 28, 2021, in the layer 10–2010 m (lower troposphere, height increment 100 m) above

Syktyvkar (a total of 54 000) for all days. The diagram thus obtained characterizes the regional probability of the transfer of air particle above the surface when moving toward the observation site in the city of Syktyvkar (Fig. 5a).

At the same time, it is known that solid precipitation falls out at a negative air temperature, T [°C], and relative air humidity, r [%], close to 100%. It was thus suggested that the regional probability of the transfer of air particles related to precipitation in Syktyvkar can be more accurately estimated by taking into account the trajectories of air particles for which $r_0 > 90\%$ and $T_0 < 0°C$ above Syktyvkar. The number of such trajectories was 17 000 from the original dataset. The regional transfer probability calculated from these trajectories is displayed in Fig. 5b. Note that the field of regional probability only insignificantly changes qualitatively when r_0 tends to 100% compared to the threshold of $r_0 = 90\%$.

We took into account only segments of the trajectories only to an hour when the specific air humidity, q [g/kg], decreases to <5% of the specific air humidity above Syktyvkar, q_0. We thus assumed that moisture transfer to Syktyvkar from areas above which $q < 0.05 \times q_0$ can be neglected. With regard to this, the regional probability is shown in Fig. 5c. Comparison of diagrams in Figs. 5a and 5b reveals their small difference, which can, in our opinion, characterize the trajectories to which the dry precipitation of aerosols between snowfalls may be related. Because both moisture and aerosol are brought to the lower troposphere from the atmospheric boundary layer (ABL) and from it to the surface, we constructed a diagram for the transfer probability analogous to Fig. 5c but for trajectory segments that occurred in the regional atmospheric boundary layer. The diagram is presented in Fig. 5d.

Diagrams in Figs. 5a–5d indicate that the formation features of the aerosol field above the urban territory on snowfall days were controlled by air particles that most probably came along an anticyclonic arc above regions on the Syktyvkar meridian (50° E) and northwestern Kazakhstan, including the northern part of the partly desertificated Aral–Caspian arid area (ACAA). The anticyclonic character of the transfer from ABL may indicate that conditions favorable for snowfalls in Syktyvkar ($r_0 > 90\%$) in winter 2021 were formed because of the invasion of the western part of the Siberian anticyclone into the European territory of Russia. The cold (Fig. 5e) and dry (Fig. 5f) air of the anticyclone, which had passed through ABL over the potentially dust-forming ACAA region and southern Russia and, hence, highly probably carried aerosol condensation nuclei, likely collided above Syktyvkar with humid (Fig. 5f) and warmer (Fig. 5e) air coming from the west. Analysis of weather conditions in an area above which air masses are transported requires a separate study, which extends outside the scope of this publication.

It should be mentioned that the character of the vertical distribution of trace elements in the snow profile (Fig. 4) provides no grounds to unambiguously extend our results to snow layers produced before February, 28. However, with regard to time periods when stratigraphically significant snowfalls occurred (Fig. 2b), we have reproduced the backward trajectories of the probability field of the transfer of air particles for underlying layers (see pair diagrams in Figs. 6a–6h). The left-hand parts of the pair diagrams in Figs. 6a–6h were calculated based on trajectories for the whole height range of 10–2010 m, whereas the right-hand ones pertain only to trajectory segments that occurred in the atmospheric boundary layer (ABL) above the city and throughout the whole lengths of the trajectories.

Analysis of the layer-by-layer diagrams (Figs. 6a–6h) led us to conclude that the chemical composition of snow layers a–e, which were formed during the time span from November 8, 2020, through December 26, 2020, were formed mostly by westerly atmospheric transfer, whereas fractions in layers f–h, which were formed starting on December 25, 2020, through February 28, 2021, were accumulated at the predominance of the easterly transfer of air masses. However, all of the studied snow layers, which grew at different trajectories of the air masses, are characterized by the dominant accumulation of the group of lithophile elements. This is clearly seen in the Gibbs–Roozeboom triangular diagram, which portrays the percentages of various components in a system of three element assemblages: lithophile elements (*Lit*) Li, Sr, Ba, Be, B, P, Sc, Ga, Ge, Y, Ti, Sn, V, and Mo–siderophile elements (*Sid*) Cr, Mn, Co, Ni, and Pd–sulfophile elements (*Slf*) Cu, Zn, Cd, Pb, and Sb. The chemical elements within the groups are similar in chemical properties, which control the general migration and concentration features of the elements in various geochemical environments. For example, siderophile elements show a strong affinity to oxygen and are prone to form metallic bonds. The activity of their migration in landscape and accumulation at reactive barriers is controlled largely by the redox conditions. The group of sulfophile elements is characterized by that these elements tend to form covalent bonds, display an stronger affinity to sulfur, and form insoluble sulfides. A common feature in the group of lithophile elements is that all of them variably tend to form ionic bonds. This readily explains the high solubility of some of their salts, their white color, and the pH of their solutions (Perel'man and Kasimov, 1999). The proportions of the three groups can be illustrated in a three-component diagram, which makes it possible to compare the concentrations of these elements and their variations from one snow layer to another and makes the results more informative (Fig. 6, inset).

Calculations show that the percentages of the three groups of elements are Lit : Slf : Sid = 74 : 11 : 14. Hence, all snow layers of the snow profile are persistently dominated by lithophile elements. In view of

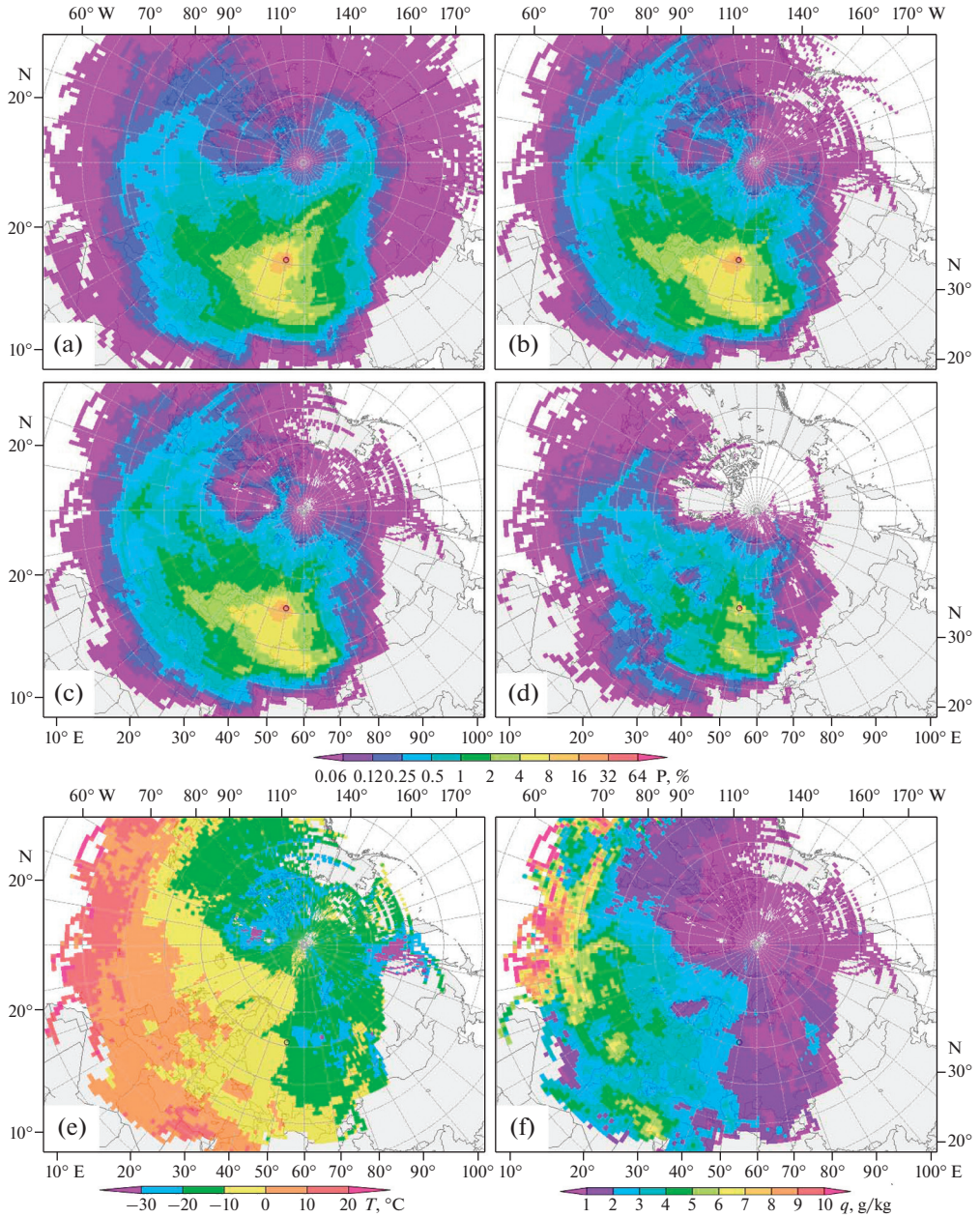

Fig. 5. Maps of the average probability, P [%], of air particle transfer above the area toward Syktyvkar (circled) in winter 2021. (a) For all trajectories in layer 10–2010 m. (b) As in (a) but for trajectories with relative humidity over Syktyvkar over 90% and a negative air temperature. (c) As in (b) but with a limitation on specific humidity (see text). (d) As in (c) but only for trajectory segments in the atmospheric boundary layer. (e) Average air temperature, T [°C], in the transfer area. (f) Average specific air humidity, q [g/kg], in the transfer area. Here and below, the cell size is 1 × 1.

this, the proportions obtained for the elemental groups in discrete snow layers and the trajectory analysis of the air masses did not allow us to unambiguously interpret these data as reflecting the winter aerosol field that was formed above the urban area as a result of long-distance transfer. Because of this, we suggest that the proportions of the groups of element assemblages in the snow layers, which were persistently preserved during the growth of the snow cover, may be used as a geochemical marker of stagnant zones in the urban heat island for ecologically–geochemically estimating atmospheric contamination at urbanized areas. It is worth mentioning that any typomorphic groups of chemical elements of the fallen out aerosol material can be used as the geochemical markers of stagnant zones in an urban heat island. Thereby the only principal requirements are that these groups of elements can be correlated with the industrial specialization of the territory and that their proportions in the snow layers were persistently preserved when the snow cover grows.

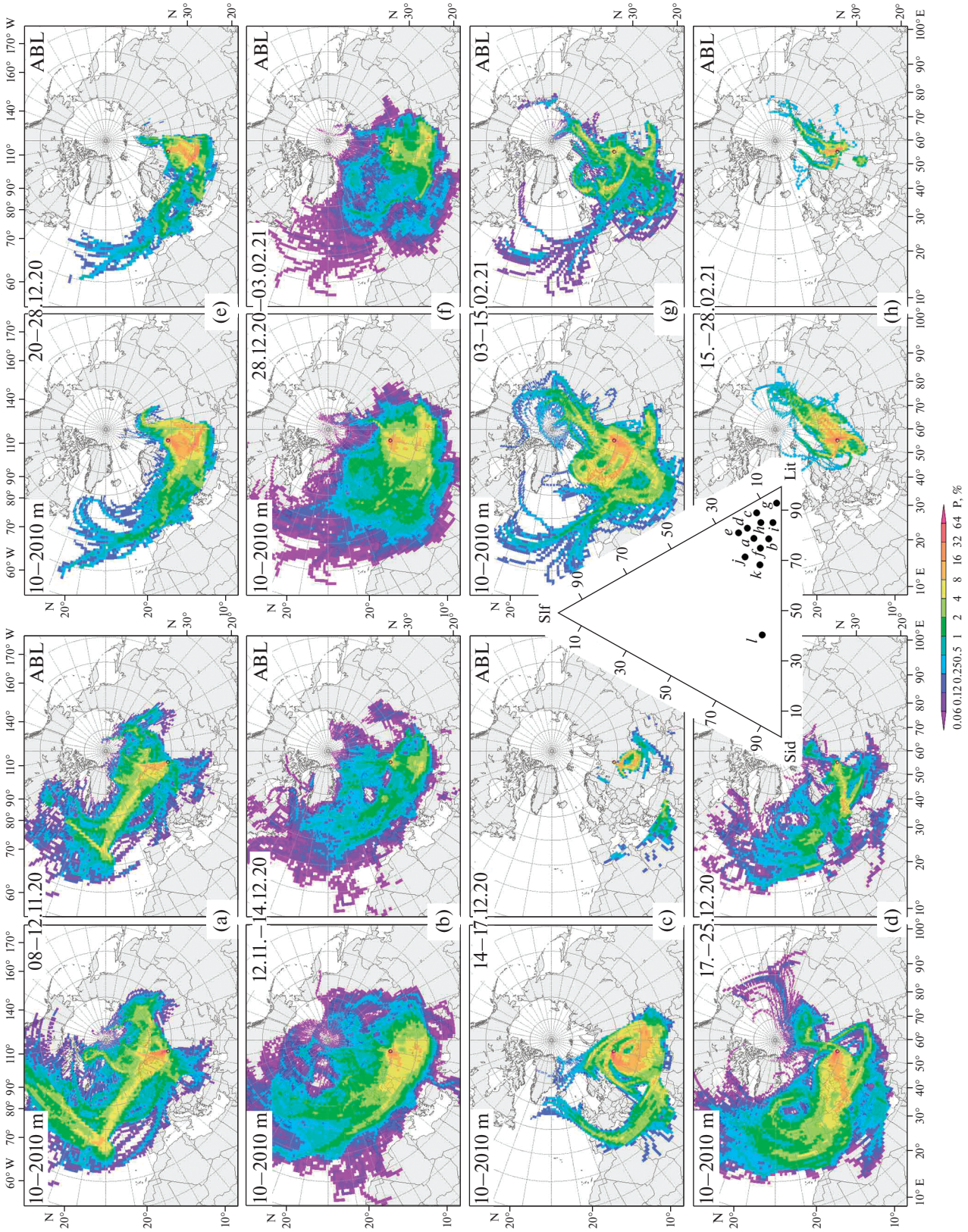
10–2010 m
ABL
08–12.11.20
12.11.–14.12.20
14–17.12.20
17.–25.12.20
20–28.12.20
28.12.20–03.02.21
03–15.02.21
15.–28.02.21
(a)
(b)
(c)
(d)
(e)
(f)
(g)
(h)
Slf
Sid
Lit
P, %
0.06 0.12 0.25 0.5 1 2 4 8 16 32 64

Fig. 6. Layer-by-layer pair diagrams for the probability of air particle transfer, P[%], at twenty levels, arriving in the layer 10–2010 m (left-hand diagrams) and within the atmospheric boundary layer (ABL; right-hand diagrams). The inset shows the distribution of elemental groups (sulfophiles, lithophiles, and siderophiles) in the snow layers chronologically correlated with the periods of stratigraphically significant snowfalls. Layers: a—December 8–12, 2020; b—December 11–14, 2020; c—December 14–17, 2020; d and e—December 17–25, 2020; f, g, h, and i—December 20–28, 2020; k—December 28, 2020–February 3, 2021; l—February 3–15, 2021; m—February 15–28, 2021.

CONCLUSIONS

Analysis of the layer-by-layer postsedimentation transformations of the granulometric composition of the fallen aerosol material in a snow profile conducted using the method of dynamic light scattering has demonstrated that aerosol material in the frost and deep frost is much more polydisperse than in the snow layers chronologically correlated with stratigraphically significant snowfalls. These features of the size distribution of parameters in ice crystals in surface and deep frost are thought to be caused by natural effects and phenomena (thermophoresis, diffusiophoresis, capillary forces, and adhesion), which are predetermined by physical properties of the snow cover.

Our comparative study of the layer-by-layer variability of the chemical composition of the fallen aerosol material allowed us to identify the proportions of three elemental groups in snow layers: siderophile elements (Sid), sulfophile elements (Slf), and lithophile elements (Lit). These proportions of element groups relatively little vary in the snow profile when the snow cover grows. Trajectory analysis of the transfer, toward Syktyvkar, of air masses to which stratigraphically significant snowfalls were related provides no grounds for explaining the detected geochemical phenomenon by that the winter aerosol field that was formed above Syktyvkar at various trajectories of air masses may be somehow inherited in snow layers of the growing snow cover and thus affect the vertical distribution of trace elements. Evidently, the proportions of the three elemental groups were found out to little vary from one snow layer to another and should reflect the occurrence of stagnant zones in the urban heat island. It should be mentioned that geochemical manifestations of the phenomenon of an urban heat island are still unknown at northern population centers, in which snow cover persists for six to eight months and longer. At the same time, a principal feature of meteorological processes in northern latitudes is a high frequency of atmospheric inversions (Nygård et al., 2014; Wetzel and Brümmer, 2011). Atmospheric boundary layers formed during such periods of time are typically stable and are characterized by the occurrence of a thin subinversion stirring layer, which facilitates the accumulation of anthropogenic heat and contaminant emissions at the air–ground interface. Their density in local zones within urban areas may reach a level at which the total solar radiation decreases and the infrared radiation from the underlying surface is shielded. Operating simultaneously and together with heat losses from living and industrial facilities, these processes result in a local greenhouse effect above the population center and in a sort of aerosol dome. Its density is sufficient to counterbalance the influence of the winter aerosol field produced over the urban area by the long-distance transfer. Because of this and despite of the different trajectories of air masses responsible for the growth of the snow cover and coming to the population center, the proportions of the elemental groups in discrete layers of the snow cover remain relatively stable.

This indicates that the proportions of elemental assemblages, which change relatively little from one snow layer to another in a growing snow cover, can be employed as a geochemical marker for the identification of stagnant zones in an urban heat island at ecological–geochemical estimations of the distribution of contaminants in the seasonal snow cover at a population center. In this context, the method proposed in this publication for geochemical study of a snow cover can be regarded as an additional tool for studying the small-scale dynamics of turbulent air flows and the transfer of contaminants in an urban environment. This tool can be efficiently utilized in combination with currently known modeling techniques in search for relations and patterns in the transfer of contaminants in urban environments and for reproducing the evolutionary dynamics of temperature anomalies (Atlaskin and Vihma, 2012; Glazunov, 2014; Anderson et al., 2015; Li et al., 2016; Sadique et al., 2017).

ACKNOWLEDGMENTS

The laser granulometry of snow slush samples was carried out at the KHIMIYA Center for the Collective Use of Analytical Equipment at the Institute of Chemistry, Komi Science Center, Ural Branch, Russian Academy of Sciences, and the composition of these samples was analyzed at the GEONAUKA Center for the Collective Use of Analytical Equipment at the Institute of Geology, Komi Science Center, Ural Branch, Russian Academy of Sciences.

CONFLICT OF INTEREST

The authors declare that they have no conflicts of interest.

FUNDING

This study was carried out under government-financed research project II.10.3.2, (registration number AAAA-A7-117021310142-5) for Zuev Institute of Atmospheric Optics, Siberian Branch, Russian Academy of Sciences, and trajectory analysis was supported by Russian Foundation for

Basic Research and the National Science Foundation of Iran, project no. 20-55-56028.

REFERENCES

W. Anderson, Q. Li, and E. Bou-Zeid, "Numerical simulation of flow over urban-like topographies and evaluation of turbulence temporal attributes," J. Turbul. **16** (9), 809–831 (2015).

E. Atlaskin and T. Vihma, "Evaluation of NWP results for wintertime nocturnal boundary-layer temperatures over Europe and Finland," Q. J. R. Meteorol. Soc. **138** (667), 1440–1451. doi.org/ (2012).1885 https://doi.org/10.1002/qj

R. R. Draxler and G. D. Hess, "An overview of the HYSPLIT_4 modeling system of trajectories, dispersion, and deposition," Aust. Meteor. Mag. **47**, 295–308 (1998).

Ecogeochemistry of Urban Landscapes, Ed. by N. S. Kasimov (Mosk. Univ., Moscow, 1995) [in Russian].

Sh. Firts, R. L. Armstrong, I. Dyuran, P. Etkhevi, I. Grin, D. M. MakKlang, K. Nishimura, P. K. Satyavali, and S. A. Sokratov, "International classification for seasonally falling snow: a guidebook to the description of snow sequence and snow cover," Proc. Glaciological Studies, No. 2, (2012).

Environmental Geochemistry (Nedra, Moscow, 1990) [in Russian].

A. V. Glazunov, "Numerical modeling of stability of stratified turbulent currents above the urban type surface. Spectra and scales, parametrization of temperature and velocity profiles," Izv. Ross. Akad. Nauk. Fiz. Atmosf. Okeana **50** (4), 406–410 (2014).

N. L. Glinka, *General Chemistry: A Textbook for Students* (Khimiya, Moscow, 1987) [in Russian].

E. E. Gurtovaya, "Some problems of temperature regime of snow cover," Role of Snow Cover in Natural Processes (Izd-vo AN SSSR, Moscow, 1961), pp. 121–131 [in Russian].

Y. -K. Hsu, T. Holsen, and P. Hopke, "Comparison of hybrid receptor models to locate PCB sources in Chicago," Atmos. Environ. **37**, 545–562 (2003).

L. S. Ivlev, "Aerosol forcing in climate processes," Opt. Atmos. Okeana **24** (5), 392–410 (2011).

L. S. Ivlev and Yu. A. Dovgalyuk, Physics of Atmospheric Aerosol Systems (NIIKh SPbGU, St. Petersburg, 1999) [in Russian].

N. S. Kasimov, D. V. Vlasov, N. E. Kosheleva, and E. M. Nikiforova, *Landscape Geochemistry of Eastern Moscow* (APR, Moscow, 2016) [in Russian].

R. Kistler, E. Kalnay, W. G. Collins, S. Saha, G. White, J. Woollen, M. Chelliah, W. Ebisuzaki, M. Kanamitsu, V. Kousky, den Dool H. van, R. Jenne, and M. Fiorino, "The NCEP–NCAR 50-year reanalysis: Monthly means CD-ROM and documentation," Bull. Am. Meteorol. Soc. **82** (2), 247–268 (2001).

E. G. Kolomyts, Theory of Evolution in Structural Snow Science (GEOS, Moscow, 2013) [in Russian].

P. P. Kuzmin, Physical Properties of Snow Cover (Gidrometeoizdat, Leningrad, 1957) [in Russian].

X. X. Li, R. Britter, and L. K. Norford, "Effect of stable stratification on dispersion within urban street canyons: A large-eddy simulation," Atmos. Environ. **144**, 47–59 (2016).

N. M. Mahowald, S. Kloster, S. Engelstaedter, J. K. Moore, S. Mukhopadhyay, J. R. McConnell, S. Albani, S. C. Doney, A. Bhattacharya, M. A.J. Curran, M. G. Flanner, F. M. Hoffman, D. M. Lawrence, K. Lindsay, P. A. Mayewski, J. Neff, D. Rothenberg, E. Thomas, P. E. Thornton, and C. S. Zender, "Observed 20th century desert dust variability: impact on climate and biogeochemistry," Atmos. Chem. Phys. **10**(22), 10875–10893 (2010).

D. V. Moskovchenko, R. Yu. Pozhitkov, and A. V. Soromotin, "Geochemical characteristics of snow cover of the town of Tobolsk," Izv. Tomsk. Politekhn. Univ. Inzhin. Geores. **332** (5), 156–169 (2021).

T. Nygård, T. Valkonen, and T. Vihma, "Characteristics of Arctic low-tropospheric humidity inversions based on radio soundings," Atmos. Chem. Phys. 14, 1959–1971 (2014). Doi:10 (2014).5194/acp-14-1959–2014

Patent 2411487. Russian Federation. MPK8 G01N1/04 (2006.01) (2011). Tentyukov snowsampler. Byul. #4. URL: https://ib.komisc.ru/files/innov/2411487.pdf. (accessed February 19, 2022).

Patent for Industrial Sample 89907, Russian Federation, MKPO10 (2014). Device for Measurement of the Heigh of Snow Cover and Increase of Frost. Byul. No. 9, (2014). URL:https://ib.komisc.ru/files/innov/89907.pdf. (accessed February 19, 2022).

A. I. Perelman and N. S. Kasimov, Landscape Geochemistry (Astreya-2000, Moscow, 1999) [in Russian].

B. R. Pinzer, M. Schneebeli, and T. U. Kaempfer, "Vapor flux and recrystallization during dry snow metamorphism under a steady temperature gradient as observed by time-lapse micro-tomography," Cryos. **6**(5), 1141–1155 (2012).

G. D. Rikhter, *Role of Snow Cover in Physicochemical Process* (Izd–vo AN SSSR, Moscow–Leningrad, 1948) [in Russian].

J. Sadique, X. I.A. Yang, C. Meneveau, and R. Mittal, "Aerodynamic properties of rough surfaces with high aspect-ratio roughness elements: effect of aspect ratio and arrangements," Bound.-Layer Meteorol. **163** (2), 203–224 (2017).

K. A. Shukurov, A. N. Borovski, O. V. Postylyakov, A. V. Dzhola, E. I. Grechko, and Y. Kanaya, "Potential sources of tropospheric nitrogen dioxide for western Moscow region," Russia. Proc. SPIE, No. 10833, 108337N (2018).

K. A. Shukurov and O. G. Chkhetiani, "Probability of transport of air parcels from the arid lands in the Southern Russia to Moscow region," Proc. SPIE, No. 10466, 104663V (2017).

S. A. Sokratov, "Parameters influencing the recrystallization rate of snow," C. R. Sci. Techn. **33** (2–3), 263–274 (2001).

S. A. Sokratov and N. Maeno, "Effective water vapor diffusion coefficient of snow under a temperature gradient," Water Resour. Res. **36**, 1269–1276 (2000).

M. P. Tentyukov, "Vosualization of Structural–textural changes in newly formed snow layer at long snow fall," Led i Sneg **61** (2), 222–231 (2021).

C. Wetzel and B. Brümmer, "An Arctic inversion climatology based on the European Centre Reanalysis ERA-40," Meteorol. Zeitschrift. **20** (6), 589–600 (2011).

Translated by E. Kurdyukov

SPELL: OK